THE JOURNAL OF BIOLOGICAL CHEMISTRY VOL. 290, NO. 50, pp. 29742–29757, December 11, 2015

Enhancing Autophagy with Drugs or Lung-directed Gene Therapy Reverses the Pathological Effects of Respiratory Epithelial Cell Proteinopathy*

Received for publication, September 9, 2015, and in revised form, October 5, 2015 Published, JBC Papers in Press, October 22, 2015, DOI 10.1074/jbc.M115.691253

Tunda Hidvegi[‡§], Donna B. Stolz[¶], John F. Alcorn[‡§], Samuel A. Yousem[‖], Jieru Wang[‡], Adriana S. Leme[**], A. McGarry Houghton[**], Pamela Hale[‡§], Michael Ewing[‡§], Houming Cai[‡§], Evelyn Akpadock Garchar[‡§], Nunzia Pastore[‡‡], Patrizia Annunziata[‡‡], Naftali Kaminski[**], Joseph Pilewski[**], Steven D. Shapiro[**], Stephen C. Pak[‡§], Gary A. Silverman[‡§¶], Nicola Brunetti-Pierri[‡‡§§], and David H. Perlmutter[‡§¶1]

From the Departments of [‡]Pediatrics, [**]Medicine, [¶]Cell Biology, and [‖]Pathology University of Pittsburgh School of Medicine and [§]Children's Hospital of Pittsburgh of UPMC, Pittsburgh, Pennsylvania 15224, [§§]Telethon Institute of Genetics and Medicine, Pozzuoli, Naples, Italy, 80131, and [‡‡]Department of Translational Medicine, Federico II University, Naples, Italy, 80138

Background: Several rare lung proteinopathies are characterized by lung fibrosis due to accumulation of misfolded proteins in epithelial cells.
Results: The PiZ mouse models the pathological characteristics of these lung proteinopathies, and the pathology is ameliorated by autophagy enhancing therapies.
Conclusion: Autophagy represents a key proteostasis mechanism for lung proteinopathies and a potential therapeutic target.
Significance: The PiZ mouse is an attractive animal model of lung proteinopathies.

Recent studies have shown that autophagy mitigates the pathological effects of proteinopathies in the liver, heart, and skeletal muscle but this has not been investigated for proteinopathies that affect the lung. This may be due at least in part to the lack of an animal model robust enough for spontaneous pathological effects from proteinopathies even though several rare proteinopathies, surfactant protein A and C deficiencies, cause severe pulmonary fibrosis. In this report we show that the PiZ mouse, transgenic for the common misfolded variant α1-antitrypsin Z, is a model of respiratory epithelial cell proteinopathy with spontaneous pulmonary fibrosis. Intracellular accumulation of misfolded α1-antitrypsin Z in respiratory epithelial cells of the PiZ model resulted in activation of autophagy, leukocyte infiltration, and spontaneous pulmonary fibrosis severe enough to elicit functional restrictive deficits. Treatment with autophagy enhancer drugs or lung-directed gene transfer of TFEB, a master transcriptional activator of the autophagolysosomal system, reversed these proteotoxic consequences. We conclude that this mouse is an excellent model of respiratory epithelial proteinopathy with spontaneous pulmonary fibrosis and that autophagy is an important endogenous proteostasis mechanism and an attractive target for therapy.

Recent studies have suggested two common pathological features for some of the diseases that we have come to recognize as "proteinopathies." For one, fibrosis is the dominant clinicopathological effect of proteinopathies in liver, skeletal muscle, heart, and lung. Intracellular accumulation of misfolded protein causes hepatic fibrosis in α1-antitrypsin deficiency (ATD)[2] (1), skeletal muscle fibrosis in inclusion-body myositis (2), myocardial fibrosis in mouse models of desminopathy (3), and pulmonary fibrosis in surfactant protein C deficiency (4–6) and Hermansky-Pudlak syndrome (7, 8). Second, autophagy appears to be a dominant proteostatic mechanism for mitigating the hepatic fibrosis in ATD (9), muscle fibrosis in inclusion-body myositis (10), and cardiac fibrosis in desminopathy (3).

Our work has focused on the classical form of ATD, an autosomal co-dominant disorder affecting ~1 in 3000 live births. A point mutation leads to misfolding of the mutant ATZ protein such that it accumulates in the endoplasmic reticulum of liver cells with decreased amounts of the protein and its anti-protease activity secreted into the blood (for review see Ref. 1). We know that intracellular accumulation of ATZ causes liver disease, hepatic fibrosis/cirrhosis and hepatocellular carcinoma, by a gain-of-toxic function mechanism (1). Some of the patients develop lung disease, and there is abundant evidence that this lung disease results from a loss-of-function mechanism in

* This work was supported, in whole or in part, by National Institutes of Health Grant HL037884 (to D. H. P.), DK084512 (to D. H. P.), DK096990 (to D. H. P.), DK079806 (to G. A. S.), HL113655 (to J. W.), and AI01953 (to J. W.), P30DK072506 (to J. P.). This work was also supported by Cystic Fibrosis Foundation R883 (to J. P.) and Telethon Foundation, Italy TCBP37TELC and TCBMT3TELD (to N. B.-P). The authors declare that they have no conflicts of interest with the contents of this article. The content is solely the responsibility of the authors and does not necessarily represent the official views of the National Institutes of Health.
[1] To whom correspondence should be addressed: Dept. of Pediatrics University of Pittsburgh School of Medicine Children's Hospital of Pittsburgh of UPMC Suite 5300, Administrative Office Bldg. 4401 Penn Ave. Pittsburgh, PA 15224. Tel.: 412-692-8071; Fax: 412-692-5946; E-mail: david.perlmutter@chp.edu.

[2] The abbreviations used are: AT, α1-antitrypsin; ATD, α1-antitrypsin deficiency; ATZ, α1-antitrypsin Z; CBZ, carbamazepine; Flu, fluphenazine; TEM, transmission electron microscopy; qPCR, quantitative PCR; COPD, chronic obstructive pulmonary disease; LTRC, Lung Tissue Research Consortium; BEC, bronchial epithelial cells; TFEB, transcription factor EB.

which proteolytic damage to the lung connective tissue results from diminished circulating levels of anti-protease (11).

In previous studies we have shown that the proteotoxic effect of ATZ accumulation in liver cells is associated with activation of the autophagic response as well as the NFκB and TGFβ signaling pathways (12–14). By counteracting the proteotoxic effect of ATZ accumulation, autophagy enhancer drugs carbamazepine (CBZ) and fluphenazine (Flu) have been found to reverse hepatic fibrosis in the PiZ model of ATD (9, 15). Furthermore, induction of autophagy in the liver of the PiZ mouse by adenoviral-mediated gene delivery of the master transcriptional regulator of the autophagolysosomal system, TFEB, reduces ATZ load and fibrosis in the liver (16). The PiZ mouse model that was used for these studies has several intriguing characteristics. It was generated with a transgene that encompassed the human ATZ gene, including exons and introns as well as upstream and downstream flanking regions (17), and it robustly recapitulates the hepatic disease of ATD (9). These mice have normal levels of endogenous antiproteases, so the liver disease must be attributable to gain-of-function mechanisms. When first analyzed, expression of mutant ATZ was detected in many extrahepatic tissues, including respiratory epithelium (17). Later AT expression in respiratory epithelium was found in another mouse model of ATD and in a human fetal lung specimen (18), leading to the conclusion that elements within the regulatory regions of the human AT gene direct AT expression in respiratory epithelial and other extrahepatic cell types. Subsequently, expression of AT has been detected in a variety of human respiratory epithelial cells as well as in bronchoalveolar macrophages by several different approaches and in a variety of cell systems (19–22).

Recently we were surprised to find significant collagen deposition in the lungs of the PiZ mice. This observation led us to hypothesize that expression of misfolded ATZ in cells of the respiratory epithelium could have the same consequences in the lung of the PiZ mouse as it has in the liver, namely gain-of-function proteotoxicity. According to this hypothesis, misfolded ATZ accumulates in respiratory epithelial cells, and one of the dysfunctional consequences is excess collagen deposition. Autophagy is also activated as a response designed to mitigate the sequelae of cellular dysfunction by degrading misfolded ATZ. However, because the endogenous autophagic response and presumably other proteostasis mechanisms are insufficient to counteract the proteinopathy, the pathological outcome is manifested by lung fibrosis, mirroring the fibrotic pathology that occurs in the liver of this mouse model. This led us to investigate here the PiZ mouse as a potential model for proteinopathies of the respiratory epithelium, such as surfactant protein C deficiency and Hermansky-Pudlak syndrome. Mouse models of these diseases have been developed, but spontaneous pulmonary fibrosis has not been yet observed, and there is still a lack of ideal models for the fibrosis that accompanies proteinopathy in the respiratory epithelium (23).

Experimental Procedures

Materials—Rabbit anti-human AT antibody was purchased from DAKO (Santa Barbara, CA), and goat anti-human AT was from Diasorin (Stillwater, MN). Other antibodies include anti-collagen I from Abcam, CD45 and F4/80 from BD Pharmingen, and ICAM1 from Abnova. CBZ and Flu were purchased from Sigma and prepared in stock solutions of 25 mg/ml DMSO and 7.5 mg/ml DMSO, respectively. The HTO/Z and HTO/M cell lines have been previously described (13). Human skin fibroblast and HepG2 cell lines were purchased from ATCC.

Transgenic Mice, Tissue, and Cells—PiZ x GFP-LC3 mice on both C57/BL6 and FVB/N backgrounds have been described previously (9). Other transgenic mice, including the ATG7-null (24), IKKβΔhep (25), and caspase 12-null (26) have also been previously described. The PiZ x GFP-LC3 mice were also bred to the Bec1-null mouse line provided by Z. Yue (27). Lung and liver from these mice were prepared for immunostaining with anti-AT and anti-GFP histochemical staining for Sirius Red; transmission and immune electron microscopy used previous methods (13). Hydroxyproline content was determined by the standard protocol (9).

For quantitative morphometric determinations, the number of stained cells, area-stained, thickness of epithelial layer or basement membrane were each quantified by blind counting in 6 microscopic fields of 10 different sections for each tissue specimen using ImageJ software. When cell counts were investigated, the number of nuclei, as determined by Hoechst staining, was used to exclude the possibility that the fields had different numbers of cells. % area stained was calculated by dividing the positively stained area by the area of the slide covered by lung tissue using the ImageJ software. These determinations are reported as the mean ± S.E.

For experiments in which mice received drug treatment with CBZ or Flu, a standard protocol with drugs administered by oral gavage 5 days per week for a total of 3 weeks, was used. Controls received a similar volume of DMSO by gavage.

Alveolar epithelial cells were isolated from PiZ and control mice using a modified version of previously established method (28). Briefly the trachea was cannulated and sterile saline instilled to rinse and remove bronchoalveolar fluid. The lungs were perfused with saline via the pulmonary artery to remove any blood. The lungs were then dissected and digested, and the lung cell suspension was obtained using Lung Cell Dissociation kit and protocol (Miltenyi Biotec, San Diego, CA). Finally, mouse type 2 pneumocytes were positively selected and purified using biotinylated anti-mouse EpCAM (e-Bioscience, San Diego, CA) with Streptavidin MicroBeads (Miltenyi Biotec, Inc.) as previously described (28). Homogenates of these cells were used to determine steady state levels of ATZ and LC3 by immunoblotting (12, 13, 29). Some of the cells were incubated with lysosomal enzyme inhibitors E-64D and pepstatin A according to previously established conditions before homogenization.

Pulmonary Function Tests—Pulmonary function was measured by the forced oscillation technique using the FlexiVent apparatus (Scireq, Montreal, QC, Canada) as previously described (30). Mice were tracheotomized with an 18-gauge cannula while under anesthesia with 90 mg/kg pentobarbital-sodium. Ventilation was carried out at 200 breaths/min at a tidal volume of 0.2 ml with a positive end-expiratory pressure of 3 cm of H_20. Multiple linear regression was used to fit pressure and volume measurements to the model of linear motion of the lung. Model fits <0.80 were excluded. Baseline measurements

of airway resistance, tissue resistance, and tissue elastance were made. In addition, pressure-volume analysis of the lung was carried out using stepwise volume inflation and deflation of the lung to a maximum pressure of 30 cm H_20. The pressure-volume data were used to calculate static lung compliance.

TFEB Gene Transfer in PiZ Mice by Nasal Instillation—The HDAd-TFEB bears the CMV promoter, driving expression of the human TFEB gene, and the HDAd-LacZ vector expresses β-galactosidase under the CMV promoter (31). The HDAd was produced in 116 cells with the helper virus AdNG163, and quality control of the viral preparations was performed as previously described (32, 33). Groups of 10 6-month-old PiZ mice were treated with HDAd-TFEB or HDAd-LacZ using a dose of 1.5×10^{10} viral particles per mouse. The viral preparation was diluted in 0.1% L-α-lysophosphatidylcholine in 0.9% NaCl to a total volume of 30 μl, and then small drops were placed in the nares as described previously (34). Mice were sacrificed 4 weeks later for analysis. To assess delivery of TFEB, relative mRNA was isolated from lung tissue and liver tissue and subjected to RT-qPCR. RNA was isolated with TRIzol reagent, and cDNA was generated using the High-Capacity RNA-to-cDNA kit from Life Technologies. Real-time PCR assays were performed using Taqman Gene Expression Master Mix in 7300 Real-Time PCR system (Applied Biosystems). Taqman probes for the human TFEB gene (Hs00292981_ml) and mouse housekeeping gene GusB (Mm00446953_ml) were purchased from Life Technologies.

Challenge of PiZ Mice with Elastase and Cigarette Smoking—For challenges with porcine pancreatic elastase and cigarette smoking we followed our previously established protocols exactly (35). Six PiZ and 6 control mice at 5 months of age received porcine pancreatic elastase. Three PiZ and 3 control mice received PBS alone as another negative control. For the smoking challenge, groups of 10 mice at 2 months of age, PiZ and control were subjected to 2 unfiltered cigarettes per day, 6 days/week for 6 months (35). We used male PiZ mice because they are known to have the highest degree of hepatic ATZ expression/accumulation and proteotoxic sequelae (9, 13). Mice from the same litter that had not been subjected to smoking were used as non-smoking controls.

Human Tissue and Cells—Explanted lung tissue specimens from six subjects with ATD were collected during lung transplantation at the University of Pittsburgh after approval by the *Institutional Review Board* with informed consent. These subjects ranged from 37 to 60 years of age and had severe progressive COPD. Ten other ATD lung specimens were provided by the Lung Tissue Research Consortium using a protocol approved by the University of Pittsburgh *Institutional Review Board*. The subjects were defined by the diagnosis of COPD with serum AT levels <80 mg/dl but more than 15 mg/dl, therein including patients likely to be ZZ or SZ allotypes but not Z-null. These patients ranged from 44 to 79 years of age and all had some history of smoking. Controls were lungs from nine subjects that did not have pulmonary disease provided by the Lung Tissue Research Consortium (LTRC) or from the Center for Organ Recovery and Education as a part of another protocol approved by the University of Pittsburgh *Institutional Review Board*. Center for Organ Recovery and Education and LTRC specimens were only used as controls if they were found to have normal morphology by blinded pathological investigation. The LTRC also provided lung tissue from three subjects with idiopathic pulmonary fibrosis.

Bronchial epithelial cells (BECs) obtained from five ATD and five normal donors were cultured on human placental collagen-coated Costar trans well filters as described previously (36). After pulse-chase radiolabeling extracellular fluid and cell homogenates were analyzed by immunoprecipitation for AT followed by SDS-PAGE/fluorography exactly as described previously (13).

Detection of AT Expression in Human Type I and Type II Pneumocytes—Human type I and II pneumocytes and alveolar macrophages were isolated from de-identified donors as previously described (37). After 6 days of culture, cells were harvested for RT-qPCR for AT (37), and supernatant was collected for extracellular levels of AT by ELISA (13).

Statistical Methods—Normality of distribution was tested with the D'Agostino and Pearson omnibus normality test. When the normality test failed, two-tailed Mann-Whitney nonparametric testing was applied. When Gaussian distribution was observed, unpaired two-tailed *t* test's were performed if variances were equal, and the same test with Welch correction was performed when the variances were different. In each case the F-test was performed to compare variances.

Software—Graphs and figures were made using Graph Pad Prism 6 and Adobe CS6. Quantitative morphometry was done using ImageJ.

Results

Expression of ATZ in the Lung of the PiZ Mouse Model Is Accompanied by Activation of Autophagy—For all of the experiments, unless otherwise noted we used the PiZ mouse bred onto the GFP-LC3 background (9) so that autophagosomes could be easily monitored, and controls were the GFP-LC3 background strain. First we investigated whether ATZ was expressed in the lung epithelial cells of PiZ mice. Type 2 alveolar epithelial cells were isolated from PiZ mice, and cell homogenates were subjected to immunoblot analysis for human AT (Fig. 1*A*). The results show the presence of an ~52-kDa polypeptide in cells from the PiZ but not control mice. An equivalent amount of the loading control GAPDH was detected in cells from control and PiZ mice. Steady state levels of ATZ in lung were ~20–25% that of the level present in the liver of PiZ mice (data not shown). To investigate whether autophagy was activated in the alveolar epithelial cells, we first subjected the homogenates to immunoblot analysis for p62, a known substrate of autophagy (Fig. 1*A*). The results show decreased levels of p62 in PiZ compared with control. To determine whether autophagic flux is increased, we subjected type 2 alveolar epithelial cells from PiZ and control mice to incubation with lysosomal enzyme inhibitors and then used immunoblot analysis to assay for LC3 isoforms (Fig. 1*B*). This is a standard assay to evaluate the flux of autophagy in that lysosomal inhibitors block the degradation of LC3-II when flux is increased (29). The results show a marked increase in LC3-II to LC3-I ratio in PiZ as compared with control and an even more profound increase in the presence of lysosomal inhibitors. These results indicate that autophagic flux is increased in lung epithelial cells of the PiZ mice.

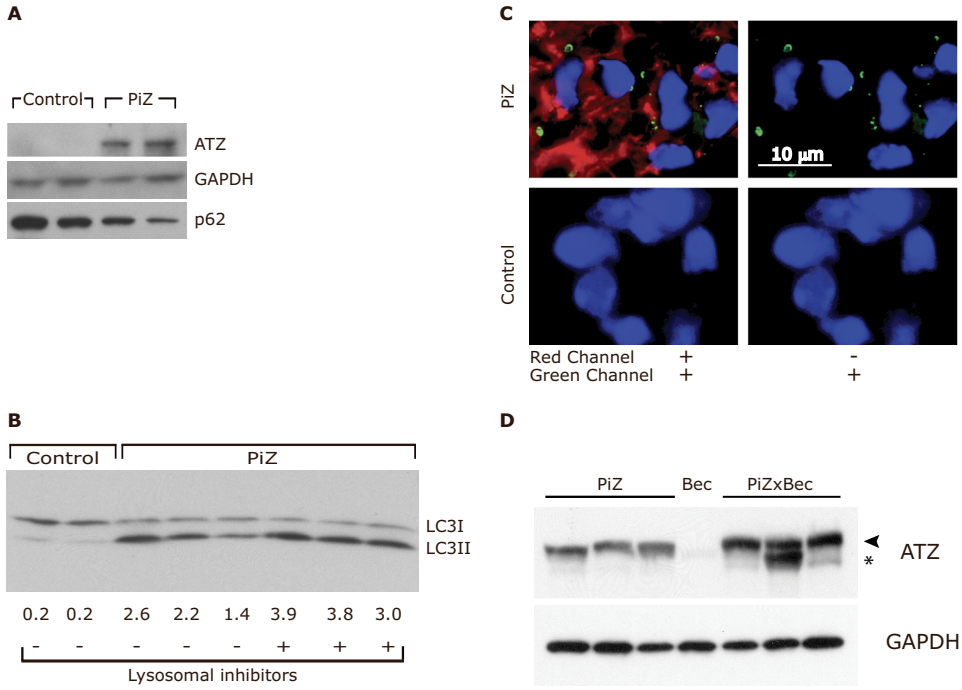

FIGURE 1. **Expression of ATZ and activation of autophagy in lungs of PiZ mice.** *A*, immunoblot analysis for ATZ, GAPDH, and p62 in alveolar epithelial cells from PiZ ($n = 2$) and control ($n = 2$) mice. In each case 50 μg protein is loaded. *B*, immunoblot analysis for LC3 isoforms in alveolar epithelial cells from control ($n = 2$) and PiZ mice ($n = 3$) after incubation in the absence (−) or presence of lysosomal enzyme inhibitors. Quantification of the LC3-II to LC3-I ratio is shown at the *bottom of the blot*. This ratio in the presence of lysosomal inhibitors was significantly increased (3.57 ± 0.28 *versus* 2.07 ± 0.30, $p = 0.0297$). A loading control is not necessary because lanes are compared with each other based on the ratio of two bands in each lane. *C*, immunostaining for AT (*red*) and LC3 (*green*) in the respiratory epithelium of PiZ x GFP-LC3 (*upper*) compared with control, GFP-LC3 mouse (*lower*). *Panels on the left* show both red and green channels, and *panels on the right* show only the green channel. Nuclei are stained *blue*. *D*, immunoblot analysis for ATZ in the lungs of PiZ ($n = 3$) and PiZ x Bec ($n = 3$) mice at age 12 months. The negative control is lung tissue from a Bec mouse. In each case 10 μg of protein is loaded. Densitometric analysis indicates that the increase in PiZ x Bec compared with PiZ is significant, $p = 0.0397$. The migration of partially and fully glycosylated ATZ is indicated at the right margin by an *asterisk* and *arrowhead*, respectively.

To further investigate whether expression of ATZ in pneumocytes is associated with activation of autophagy, we subjected sections of lung from PiZ and control mice to double-label immunostaining with anti-AT (*red*) and with anti-GFP (*green*) to detect GFP+ autophagosomes (Fig. 1*C*). The PiZ x GFP-LC3 mouse is shown in the *top panels*, and the control GFP-LC3 mouse is shown in the *bottom panels*; the merged image for both *red* and *green* fluorescence is on the *left* and for *green only* is on the *right*. The results show accumulation of ATZ in the PiZ mouse (*upper left*) but not control (*lower left*). GFP+ vacuoles are seen in the cells that are positive for ATZ accumulation (*upper left*), and this can be seen even more clearly when viewed through the green channel in the *upper right panel*. No staining for ATZ or GFP was seen in the controls (*lower panels*). These results show ATZ expression in epithelial cells and autophagosomes within the same cells. Furthermore, they show that ATZ expression is sufficient to activate autophagy because autophagosomes are not present in the control GFP-LC3 mouse in the *lower panels*. It is known that GFP+ autophagosomes are only seen in the GFP-LC3 mouse when autophagy is activated by starvation (12, 38).

To determine whether autophagy plays a role in disposal of ATZ in the lungs of the PiZ mouse model, we examined the levels of ATZ in the PiZ x Bec mouse model (Fig. 1*D*). The Bec mouse model is heterozygous null for beclin 1 in all tissues and therein is partially deficient in autophagy (27, 39). The 52-kDa ATZ polypeptide could be detected in homogenates of whole lung tissue. It was specific as shown by the lack of any signal in the Bec mouse. Most importantly, ATZ levels were increased in the PiZ x Bec mice compared with the PiZ mice (the increase was statistically significant by densitometric analysis, $p = 0.0397$). Indeed both the mature and a partially glycosylated form of ATZ accumulated in the lung of the PiZ x Bec mice. These results provide evidence that ATZ accumulation increases when autophagy is partially deficient.

Together, these results provide evidence that expression of misfolded ATZ in respiratory epithelial cells of the PiZ mouse is accompanied by activation of autophagy with increased autophagic flux, characteristic of what occurs in the liver in the PiZ mouse and in humans with ATD and in inclusion-body myositis and cardiac desminopathy. Furthermore, the results indicate that autophagy plays a role in preventing even more accumulation of misfolded ATZ in the lung.

Excess Collagen Deposition, Leukocyte Infiltration, and Stiffening in the Lungs of the PiZ Mouse Model—Next we investigated the possibility that collagen deposition was increased in the lungs of the PiZ mice. Using trichrome staining (Fig. 2*A*), there is a marked and statistically significant increase in collagen deposition throughout the lungs, including alveolar septal walls and around airways (% area stained was 9.83 ± 0.92 for PiZ and 2.83 ± 0.41 for control, $p < 0.0001$). Collagen I immunostaining also demonstrated a marked and significant increase in the PiZ mice (PiZ 8.02 ± 0.99 $n = 12$; control 0.08 ± 0.02, $n = 12$; $p < 0.0001$ by two-tailed Mann-Whitney test). Hydroxypro-

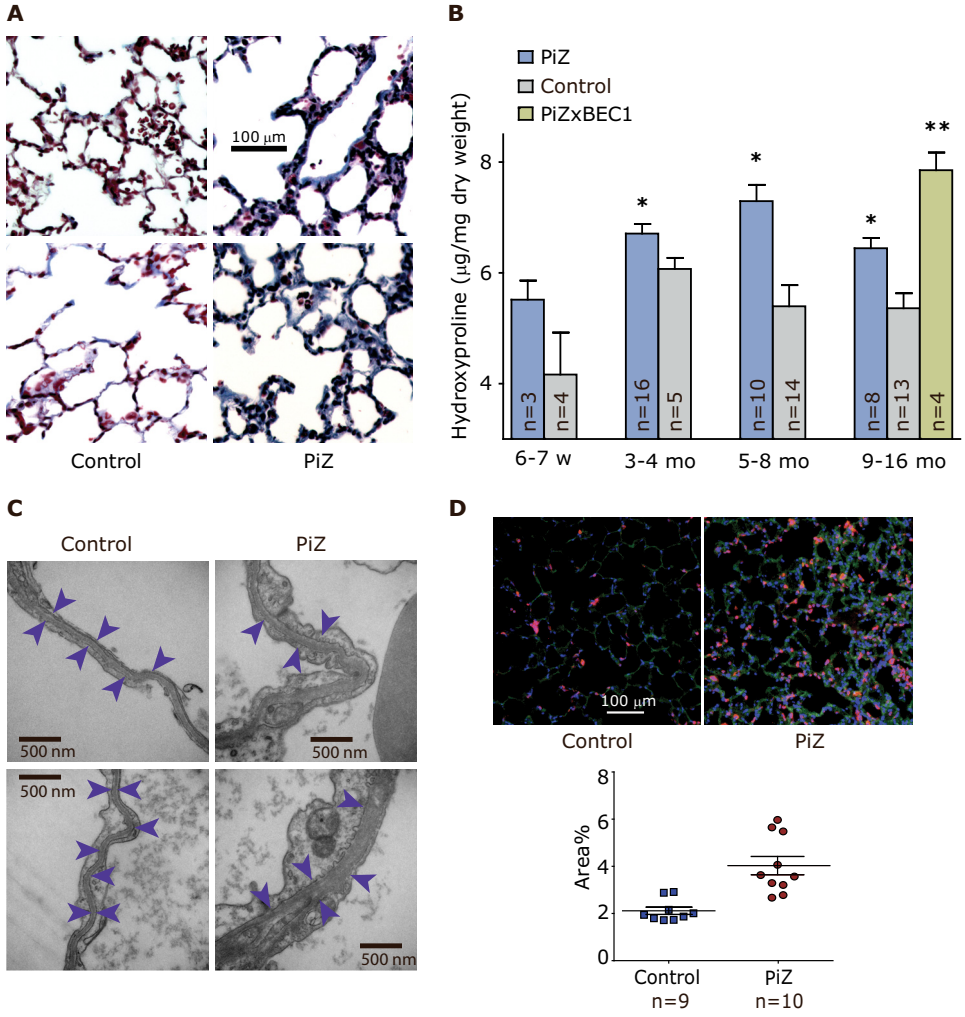

FIGURE 2. **Collagen deposition and leukocyte infiltration in lungs of PiZ mice.** *A*, histochemical staining with trichrome. PiZ x GFP-LC3 ($n = 2$) is in the *right panels*, and control, GFP-LC3 ($n = 2$), age 6 months, is in the *left panels*. % area stained was 9.83 ± 0.92 for PiZ-GFP-LC3, $n = 61$ *versus* 2.83 ± 0.41 for control, $n = 21$; $p < 0.0001$). *B*, hydroxyproline content. The mean ± S.E. is shown for each group ($n = 5–8$). *, difference from control, $p < 0.005$; **, difference from PiZ, $p < 0.005$. *C*, TEM imaging. Sections from 2 mice each at 50,000× magnification. The thickness was significantly increased in PiZ ($n = 6$) *versus* control ($n = 5$) at age 6–12 months analyzing 27 and 25 fields, respectively ($p < 0.0001$). The *arrows* point to basement membrane. The control in each is GFP-LC3. *D*, immunostaining of leukocytes in the lungs of PiZ mice using anti-CD45 (*pink*). Quantitative morphometry was done for PiZ ($n = 4$) and the control ($n = 3$) at age 6 months, analyzing 10 and 9 fields, respectively, for % area stained in sections shown as the mean ± S.E. $p = 0.0006$ at the *right*. The control was GFP-LC3.

line quantification also demonstrated excess collagen deposition in the lungs of PiZ mice at 3–4, 5–8, and 9–16 months. It was also increased at 6–7 weeks, but this increase did not reach statistical significance (Fig. 2*B*). It is important to note that the increase in the PiZ lung hydroxyproline content reached 158% that of control in the 5–8 months age group, a magnitude that is comparable with what has been reported for bleomycin-induced pulmonary fibrosis (40). Furthermore, lung hydroxyproline content was significantly increased in PiZ mouse that were bred onto the beclin1-heterozygous null background (PiZ x Bec1) when compared with the PiZ mouse (Fig. 2*B*). These results suggest that partial deficiency of autophagy renders the PiZ mouse more susceptible to lung collagen deposition and, therein, provides further evidence that autophagy ordinarily counteracts a fibrogenic process in the lung. Lung hydroxyproline content was significantly increased in PiZ mice compared with 5 separate groups of controls (hydroxyproline content (μg) in PiZ 0.16 ± 0.01, $n = 6$; controls *versus* PiZ compared by two-tailed t test: wild-type 0.07 ± 0.01 $n = 20$, $p = 0.0002$; ATG7-null 0.06 ± 0.01 $n = 4$ $p = 0.0002$; beclin1 heterozygotes 0.06 ± 0.00 $n = 4$ $p = 0.0002$; caspase12-null 0.07 ± 0.01 $n = 5$ $p = 0.001$; IKKβ kinase null 0.07 ± 0.01 $n = 4$ $p = 0.0004$), providing evidence that it was not a strain-specific effect. TEM also demonstrated marked thickening of the basement membrane in proximal and distal airways (Fig. 2*C*). Quantitative morphometry of the thickness of the entire epithelial layer and of the basement membrane alone showed highly significant differences between PiZ and control lungs using the two-tailed Mann Whitney test (epithelial layer PiZ 539.7 nm ± 39.89 $n = 15$, control 257.7 nm ± 29.85 $n = 19$, $p < 0.0001$; basement membrane PiZ 153.5 nm ± 11.98 $n = 27$, control 71.04 nm ± 3.26 $n = 25$ $p < 0.0001$). Thus, the PiZ mouse model has a robust spontaneous pulmonary fibrosis response as reflected by four different types of analyses.

Next we investigated whether the lung phenotype in the PiZ mouse model includes leukocyte infiltration by subjecting lung specimens from PiZ mice to immunostaining for the pan-leukocyte marker CD45 (Fig. 2*D*). The results show a marked

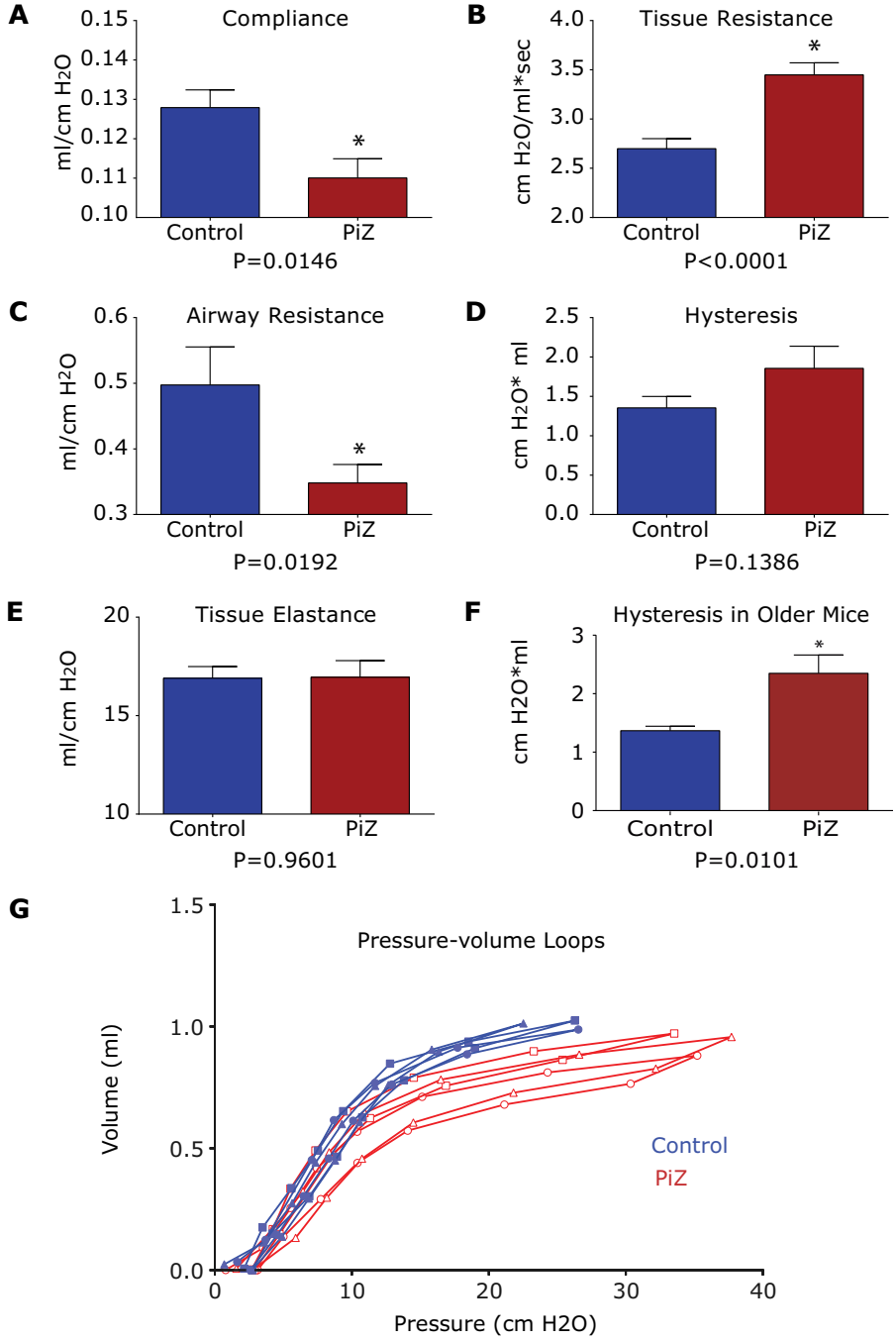

FIGURE 3. **Pulmonary function test in PiZ mice.** Lung compliance (*A*), tissue resistance (*B*), airways resistance (*C*), hysteresis (*D*), and tissue elastance (*E*) are shown for PiZ ($n = 13$) and wild type ($n = 11$) at 9 months of age. Hysteresis is also shown for PiZ ($n = 11$) and wild type ($n = 8$) at 15–18 months of age (*F*), *Bars* represent the mean ± 1.0 S.E., and *p* values are shown at the *bottom of each panel*. *Asterisks* indicate statistically significant difference from control. In *G*, pressure-volume loops for three representative PiZ and three control mice are shown.

increase in CD45+ cells infiltrating the lungs. F4/80 immunostaining for macrophages was not increased (PiZ 1.87 ± 0.13 $n = 12$, control 0.94 ± 0.13 $n = 12$, $p = 0.4507$ by two-tailed Mann-Whitney test), suggesting that the infiltration is predominantly composed of neutrophils and/or lymphocytes. There was a significant increase in staining for ICAM1 (PiZ 6.20 ± 1.34 $n = 12$, control 1.30 ± 0.24 $n = 12$, $p < 0.0001$, by two-tailed Mann-Whitney test), suggesting endothelial activation that is seen in lung inflammation. These results indicate that leukocyte infiltration is another marker of lung involvement in this model of respiratory epithelial cell proteinopathy.

Next we investigated whether these pathological changes have a significant physiological effect, such as lung stiffening, using the Flexivent apparatus to measure pulmonary function by the forced oscillation technique. We used older mice, (9 months of age) based on a presumption that collagen deposition was progressive and compared PiZ mice to controls (Fig. 3). The results demonstrate a significant reduction in compliance (14.1%; Fig. 3*A*) and a marked increase in tissue resistance (28.8%; Fig. 3*B*) in the PiZ mice, consistent with the type of stiffening that would be observed with pulmonary fibrosis. Interestingly, there was also a marked decrease in airways resis-

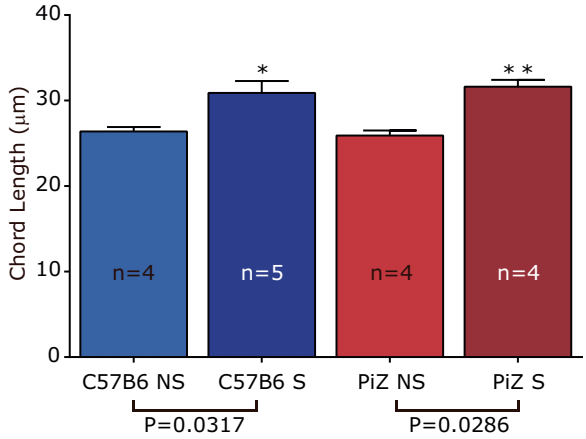

FIGURE 4. **Cigarette smoking challenge of PiZ compared with C57B6 mice.** Groups of male mice were subjected to cigarette smoking (*S*) from 2 to 8 months of age and compared with equal numbers of mice that were not smoked (*NS*). Chord length was significantly increased by cigarette smoking, $p = 0.0317$ for C57B6 (*) and $p = 0.0286$ for PiZ (**). There were no significant differences for PiZ NS *versus* C57B6 NS ($p = 0.4857$) and PiZ *versus* C57B6 S ($p = 0.4440$), two-tailed Mann-Whitney test.

tance (30%; Fig. 3*C*), probably reflecting that airways are more effectively held open when the lung interstitium is stiffened by excess collagen (41). Hysteresis was increased in the PiZ mice, but this difference did not reach statistical significance (Fig. 3*D*). However, the increase in hysteresis reached statistical significance in PiZ mice at 14–17 months of age compared with age-matched controls (Fig. 3*F*). Furthermore, the pressure-volume loops were shifted downward and to the right (Fig. 3*G*), a pattern of altered hysteresis indicative of the requirement for higher pressures to achieve the same lung volume and identical to what has been described in patients with idiopathic pulmonary fibrosis (42). There was no significant difference in tissue elastance (Fig. 3*E*). These results indicate that collagen deposition is sufficient to affect the physiological phenotype of the PiZ mice with increased lung stiffening. From our review of the literature there are no other mouse models with spontaneous collagen deposition severe enough to cause restrictive functional deficits. Furthermore, the profile of changes in lung function that occur spontaneously in the PiZ model are almost identical to what occurs in human diseases with pulmonary interstitial fibrosis, and the magnitude of these changes is comparable to what is reported for the bleomycin-induced model of experimental pulmonary fibrosis (40, 43–45).

PiZ Mice Are Not Susceptible to Emphysema Induced by Challenge with Elastase or Cigarette Smoking—To further characterize the lung phenotype in PiZ mice we examined them for emphysematous changes. There was no evidence for spontaneous emphysema in routine histological examination of the PiZ lungs. Challenge with cigarette smoking resulted in increased chord length in the lungs of smoked male PiZ mice compared with un-smoked PiZ mice, and that increase was indistinguishable from what occurred in the control mice (Fig. 4). Elastase challenge also showed no difference. These data indicate that PiZ mice are not more susceptible to emphysema, consistent with the concept that emphysematous pathology in ATD is due to loss-of-function and that the PiZ model does not manifest pathological effects due to loss-of-function.

Effect of Delivering Autophagy-activating Transcription Factor TFEB on Pulmonary Collagen Deposition and Leukocyte Infiltration Using Lung-specific Gene Transfer—Next we investigated the effect of activating the autophagic response locally by lung-directed expression of TFEB, the master transcriptional activator of the autophagolysosomal system (16, 46). We used an HDAd vector expressing TFEB under the control of the CMV promoter to achieve broad expression in the respiratory epithelium, and the vector was administered to PiZ mice by nasal instillation. An HDAd vector expressing the LacZ reporter gene under the control of the same CMV promoter was used as the control to exclude nonspecific effects of double-stranded DNA. The results show that TFEB gene transfer mediates a significant reduction in collagen deposition, as determined by collagen I immunostaining (Fig. 5*A*) and Sirius Red staining (Fig. 5*B*) and a significant reduction in leukocyte infiltration as measured by CD45 staining (Fig. 5*C*). Furthermore, there was a significant decrease in steady state levels of ATZ in the lungs of the TFEB-treated mice (Fig. 5*D*). This a very important result because it provides evidence that reduced ATZ load is linked to reduced pathology in the lung as a result of TFEB gene transfer and expression. Several other results validate the specificity of this series of experiments. First, there was no difference in hepatic collagen deposition as determined by Sirius Red staining and hydroxyproline content (data not shown) or hepatic ATZ load as determined by PAS/diastase staining (data not shown). Second, human TFEB expression was detected by RT-qPCR in the lungs of the PiZ mice that received the TFEB expressing vector but was undetectable in the lungs of the PiZ that received the control vector and was undetectable in the livers of both groups (data not shown). These results indicate that expression of the autophagy-activating transcription factor TFEB in the airway epithelium specifically reduces ATZ load and proteotoxic sequela in the lung of the PiZ mouse model.

Effect of Autophagy Enhancer Drugs on Pulmonary Collagen Deposition, Stiffening, and Leukocyte Infiltration—Next, we addressed the hypothesis that, by reducing ATZ accumulation/proteotoxicity, autophagy enhancer drugs would influence collagen deposition and leukocyte infiltration in the lungs of the PiZ model. PiZ mice at 3 months of age were treated for 3 weeks with autophagy enhancers CBZ 100 mg/kg/day and Flu 7.5 mg/kg/day. Collagen deposition was shown to be significantly decreased by drug treatment as evaluated by two different assays. First immunostaining for collagen I (Fig. 6*A*) showed a marked and statistically significant decrease in the lungs of mice treated with CBZ/Flu (% area for placebo 26.81 ± 0.96, $n = 35$ images *versus* CBZ/Flu 23.31 ± 1.090, $n = 37$ images; $p = 0.018$). Second, lung hydroxyproline content was significantly decreased in PiZ mice treated with CBZ/Flu (placebo 4.98 ± 0.36, $n = 7$ mice *versus* CBZ ± Flu 4.04 ± 0.07 μg/mg tissue, $n = 5$ mice; $p = 0.0355$). Furthermore, CBZ and Flu each profoundly decreased leukocyte infiltration (Fig. 6*B*; placebo 3.034 ± 0.397, $n = 30$ *versus* CBZ/Flu 1.911 ± 0.163, $n = 34$; $p = 0.0127$ by *t* test).

Last, we tested the effect of autophagy enhancer drugs on lung stiffening in the PiZ mice (Fig. 6*C*). In this case we used older mice (12–14 months old) so that the effect of the drugs on the most advanced phenotype could be determined. Placebo ($n = 11$) or the combination of CBZ and Flu ($n = 12$) was

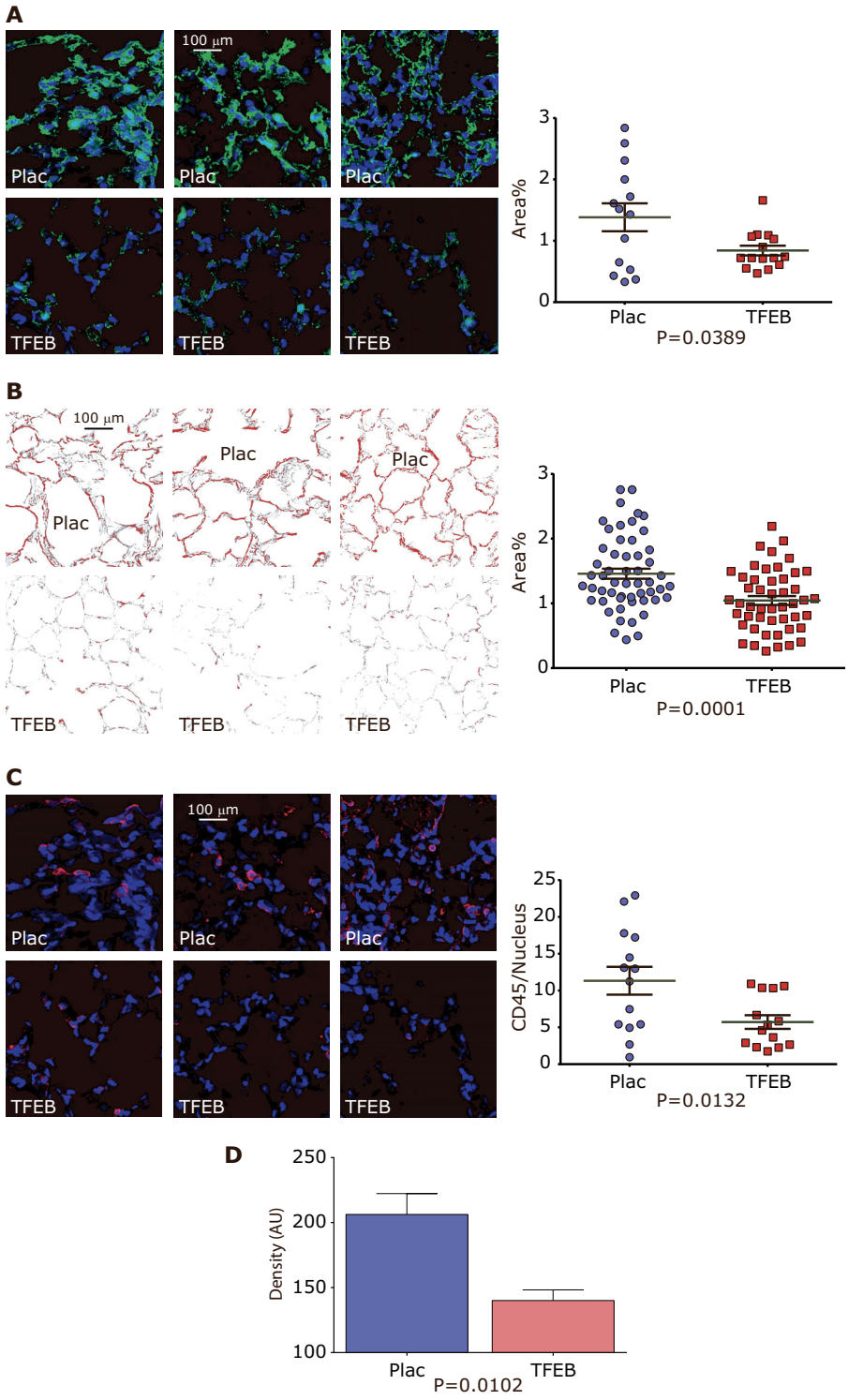

FIGURE 5. **Effect of lung-directed TFEB gene transfer on lung collagen deposition and leukocyte infiltration.** *A*, collagen I immunostaining. *B*, Sirius Red staining. *C*, CD45 staining. Morphometric results and *p* values are shown to the *right of the images*. The mice were age 24 months, $n = 9$ for each group. The number of fields analyzed were 15 and 14 for *A*, 48 and 54 for *B*, and 14 each for *C*. *D*, ATZ levels as determined by densitometric scanning of immunoblots. The mice were age 24 months, $n = 4$, for TFEB, $n = 3$ for control. *AU*, absorbance units.

administered by subcutaneous pellets for 6 weeks. The results show a marked and statistically significant reduction in tissue resistance. In fact the tissue resistance was reduced to the level of wild type mice (see Fig. 3). CBZ and Flu treatment also led to a statistically significant reduction in hysteresis (Fig. 6*C*), and the pressure-volume loops shifted toward the left and upward (Fig. 6*D*). When compared with placebo and overlaid on the loops from wild type and PiZ mice (data from Fig. 3) it can be seen that the treatment corrected the pattern of the pressure-volume curve almost back to the pattern of wild type mice (Fig. 6*D*). The treatment did not reverse the pathological changes in lung compliance and airway resistance in this series of experi-

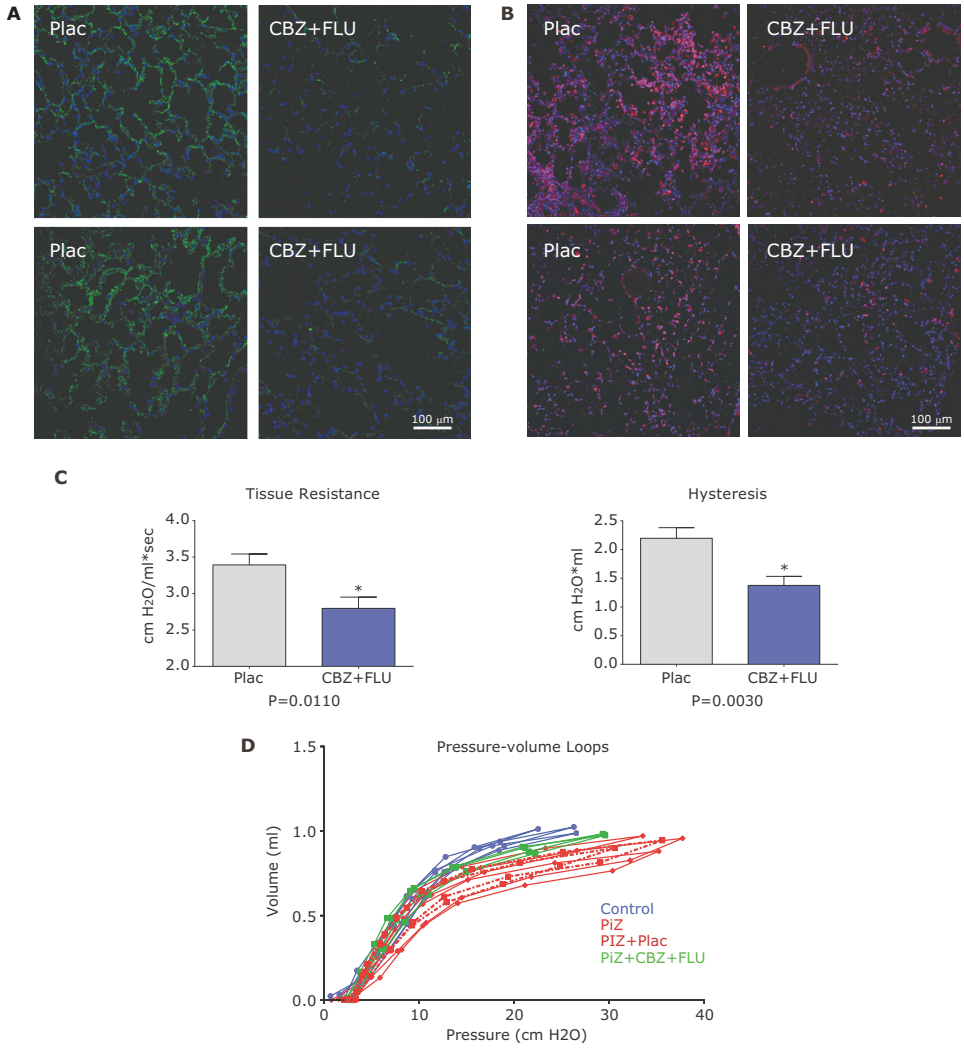

FIGURE 6. **Effect of autophagy enhancer drugs on lung collagen deposition, lung leukocyte infiltration, and lung function in PiZ mice.** *A*, immunostaining for collagen I in lung. PiZ mice at 3 months of age ($n = 19$ in each group) were treated for 3 weeks with placebo or both CBZ 200 mg/kg/day and Flu 7.5 mg/kg/day by oral gavage. *B*, immunostaining for CD45 from same specimens used for *A*. Quantitative morphometry for 30–37 fields in each case was expressed as mean ± S.E. is shown on the *right* of *A* and *B*. *Asterisks* indicate a statistically significant difference from placebo. *C*, pulmonary function tests. PiZ mice at 12–15 months of age were treated with placebo ($n = 5$) or CBZ 200 mg/kg/day and Flu 7.5 mg/kg/day ($n = 7$) for 6 weeks. *Bars* represent the mean ± 1.0 S.E. *Asterisks* indicate statistically a significant difference from placebo. *D*, pressure-volume loops for representative PiZ mice treated with placebo ($n = 2$; *dark red*, *dots and dashes*) and for representative PiZ mice treated with CBZ and Flu ($n = 2$; *green*) are shown overlaying pressure-volume loops for representative wild type (*light blue*) and PiZ mice (*light red*) from the experiments of Fig. 3.

ments. It may be that earlier initiation and/or longer duration of therapy is needed to reverse the decreases in compliance and airway resistance that reflect altered lung function in the PiZ mice. CBZ/Flu had no effect on the pulmonary function of control mice (data not shown). Together, these results indicate that autophagy enhancer drugs CBZ and Flu mediate significant reductions in lung collagen deposition, leukocyte infiltration, and at least two measures of lung stiffening in the PiZ model.

Expression of ATZ in Human Respiratory Epithelial Cells Is Accompanied by Increased Autophagic Flux—Next we investigated whether AT is expressed in respiratory epithelial cells from human lung and whether misfolded ATZ accumulates with activation of autophagy in these cells. First, type I and II pneumocytes as well as pulmonary macrophages cultured from normal human lung were found to express AT by RT-qPCR and ELISA (Fig. 7). Second, BECs were cultured from the native lungs of patients with ATD who underwent lung transplantation. BECs were used because they are the only epithelial cells available from human lungs. Pulse-chase labeling for analysis of synthesis and secretion (Fig. 8*A*) shows that BECs from the control (*MM*) have the characteristic ~52- and 55-kDa polypeptides in the intracellular lysates (*IC*) and the mature 55-kDa polypeptide in the extracellular fluid (*EC*). These results are very similar to what is seen in a HeLa cell line genetically engineered for expression of wild type AT, the HTO/M cell line (13) shown in the *right panel*. In the BECs from the ATD patient (ZZ) only the ~52-kDa polypeptide is present in the intracellular lysate, and very little if any of the mature 55-kDa polypeptide is found in the intracellular lysate or extracellular fluid, results almost identical to what is seen in the genetically engineered HTO/Z cell line in the *right panel* (13). These data were representative of what was observed in four different patients with ATD and provide evidence for expression of ATZ with its char-

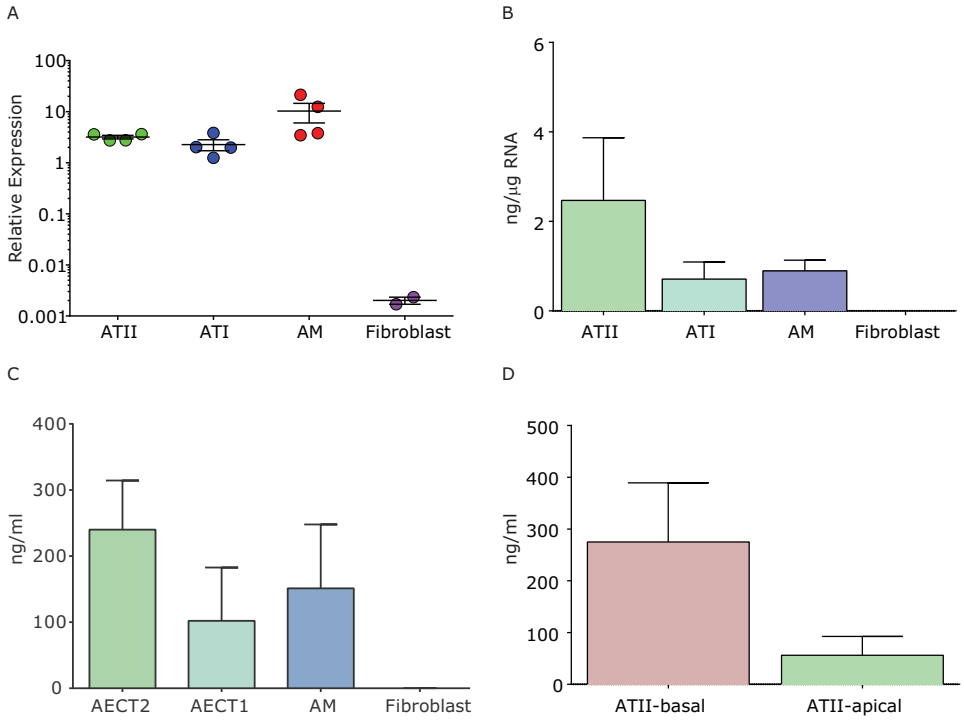

FIGURE 7. **Relative AT RNA and protein levels in human respiratory epithelial cells and alveolar macrophages.** Relative expression of AT was determined by RT-qPCR and ELISA in cultures of type II pneumocytes (*ATII*, AECT2), type I pneumocytes (*ATI*, AECT1), and alveolar macrophages (*AM*) isolated from human lung. The negative control was a human skin fibroblast cell line. *A*, RNA levels. *B*, protein levels in ng/μg RNA. *C*, protein levels in ng/ml. *D*, protein levels in basal *versus* apical extracellular fluid.

acteristic defect in biogenesis in at least one lung epithelial cell type from the patients.

We also investigated the possibility that autophagy was activated in BECs from ATD patients. When compared with control, there was a marked decrease in p62 levels (Fig. 8*B*) and an increase in the LC3-II/LC3-I ratio (Fig. 8*C*). Furthermore, the LC3-II/LC3-I ratio was further and markedly increased in the presence of lysosomal enzyme inhibitors, indicative of a marked increase in autophagic activity/flux.

Last, TEM imaging of native lung tissue from six patients with severe, early onset lung disease due to ATD showed dilated endoplasmic reticulum associated with autophagosomes in respiratory epithelial cells and could be seen in both type I (Fig. 9) and type 2 pneumocytes. Together these results indicate that the proteinopathy observed in respiratory epithelial cells of the PiZ mouse is also seen in human respiratory epithelial cells and that it is significant enough to cause morphological changes and increased autophagic flux in at least some patient specimens.

Excess Collagen Deposition in Human ATD Lungs—Next, we investigated whether excess collagen was deposited in lung tissue from ATD patients. Fibrosis is not mentioned in most descriptions of ATD (47), but lung tissue specimens from patients with COPD are not routinely subjected to histochemical staining for collagen, and recent studies suggest that it can be detected in some cases of COPD by sophisticated analyses (48–50). In six ATD patients with severe lung disease, TEM showed profound collagen deposition throughout the lung parenchyma, in alveolar septal walls as well as deposited adjacent to proximal and distal airways and within thickened basement membranes (Fig, 10). When these 6 ATD patients were compared with 9 normal controls by quantitative morphometry, the percent area occupied by collagen (ATD 24.82 $\pm$ 2.21 $n = 16$, normal 5.126 $\pm$ 0.787 $n = 10$) and the thickness of the basement membrane (ATD 0.468 μm $\pm$ 0.014 $n = 91$, normal 0.352 μm $\pm$ 0.016 $n = 54$) were significantly increased in ATD specimens ($p < 0.0001$ two-tailed t test with Welch correction and two-tailed t test, respectively). Moreover, immunostaining for collagen I showed significantly increased staining in the ATD lungs (22.88 $\pm$ 0.84, $n = 7$) compared with normal controls (10.31 $\pm$ 1.134, $n = 10$), $p < 0.0001$ by two-tailed Mann-Whitney test. Next we received from the NHLBI, National Institutes of Health-funded LTRC 10 lung tissue specimens from ATD individuals with COPD and 3 lung tissue specimens from individuals with idiopathic pulmonary fibrosis as positive controls. The 16 ATD specimens, 3 idiopathic pulmonary fibrosis specimens, and 9 normal controls were subjected to Masson's trichrome staining and analyzed blindly by a lung pathologist (S.A.Y.) using a scale of 0–4 for the degree of staining. In Fig. 11, *left panel*, several examples of normal controls and ATD specimens show that there is a significant increase in trichrome staining (*blue*) in the alveolar septal walls and airways of the ATD tissue. The results of the blinding scoring are shown in Fig. 11, *right panel*, and indicate that trichrome staining is significantly increased in ATD compared with normal, $p = 0.0118$. All 3 of the idiopathic pulmonary fibrosis specimens were scored as 4+. A total of 13 of 16 ATD patients had staining that was scored 1+ to 3+. Four of the 16 ATD patients scored 3+. Although pulmonary function results are collected by the LTRC, there was an insufficient number of the ATD individuals with full pulmonary function results that would permit us to determine any correlation between degree of trichrome staining and restrictive functional deficits. Never-

theless, these data indicate that excess collagen deposition is present in the lungs of patients with ATD, and the degree of collagen deposition is moderately severe in a subgroup. Because collagen deposition may occur in humans with ATD for other reasons, including cigarette smoking and as a part of bronchiectasis, it is not possible to determine whether this pathological characteristic in human lung specimens is wholly, or even in part, due to the proteinopathy mechanism.

Discussion

The results of this study indicate that the PiZ mouse provides an attractive model for respiratory epithelial proteinopathies and has the unique characteristic of excess collagen deposition that occurs spontaneously. Previous studies have suggested that AT is synthesized in respiratory epithelial cells (18–22) and mutant ATZ was detected in respiratory epithelium of the PiZ mouse (17). We confirmed the concept that AT is synthesized in type I and type 2 pneumocytes and that misfolded ATZ accumulates in pneumocytes from the PiZ mouse as well as bronchial epithelial cells from patients with ATD. Furthermore we demonstrate that the accumulation of misfolded ATZ in pneumocytes has cellular consequences consistent with a proteotoxic effect, *i.e.* activation of autophagy with increased autophagic flux, identical to what occurs in liver cells in ATZ (9) and other cell types affected by proteinopathies (3, 10). The increase in lung collagen deposition models the clinicopathological characteristics of several genetic diseases, including surfactant protein C deficiency (4–6), surfactant protein A deficiency (51), and Hermansky-Pudlak syndrome (7, 8). Although expression of mutant surfactant protein C in genetically engineered mice produces increased susceptibility to fibrotic stimuli (5, 52), existing mouse models of these genetic diseases do not develop pulmonary fibrosis spontaneously (for review, see Ref. 23). In the PiZ mouse model the excess collagen deposition was not only spontaneous but was severe enough to produce significant and highly specific changes in pulmonary function, including decreased lung compliance, increased lung tissue resistance, decreased airway resistance, and altered hysteresis, consistent with a pure restrictive phenotype. The fibrotic effects were defined by clearly measurable outcomes including trichrome staining, Sirius Red staining, collagen I immunostaining, hydroxyproline content, and a demonstrable infiltration of CD45-stained cells. The magnitude of changes that defined each of these outcomes was in the range of, if not comparable to, what has been seen in the bleomycin models of pulmonary fibrosis (40, 43–45). We can imagine two potential reasons for why this phenotype is manifested in the PiZ mouse model and not in previous models of respiratory epithelial cell proteinopathy; overexpression of misfolded ATZ is an artifact of transgenic "overexpression" in the PiZ mouse, or AT is expressed at higher levels physiologically in respiratory epithelial cells than surfactant proteins A or C. The high levels of expression of AT detected in human type I and type 2 pneumocytes (Fig. 7) and the clear-cut evidence for accumulation of ATZ in bronchial epithelial cells to levels that increase autophagic flux (Fig. 8) led us to believe that the spontaneous fibrotic phenotype in the PiZ mouse is due to the second explanation, higher levels of expression physiologically.

A number of previous studies have indicated that autophagy plays a critical role in degradation of ATZ. Degradation of ATZ was impaired in autophagy-deficient ATG5-null murine embryonic fibroblasts (12). ATZ co-localized with LC3 in a mammalian cell line model expressing a dominant-negative Rab that inhibits autophagosomal maturation (12) and ATZ co-localized with LGG, the *Caenorhabditis elegans* ortholog of LC3, by live organism imaging in a *C. elegans* model expressing GFP-ATZ and RFP-LGG chimeras (53). Two series of results in this study show that autophagy also contributes to degradation of ATZ in the lung. First, steady state levels of ATZ in the lung were significantly increased in the PiZ x Bec mice with partial deficiency in autophagy compared with PiZ mice (Fig. 1*D*). Second, levels of ATZ decreased in the lung of PiZ mice who received lung-directed gene transfer of TFEB, the master transcriptional activator of the autophagolysosomal system.

This study also provides additional evidence for the importance of the autophagic response as a proteostatic mechanism in lung proteinopathies as has been shown for other tissues (3, 9, 10). Autophagy is increased in lung epithelial cells from PiZ mice and humans. Lung pathology is worsened when the autophagic response was partially impaired and almost completely eliminated when autophagy was enhanced either by systemic drug therapy or lung-directed gene therapy. Although further studies in which expression of ATZ and the autophagic response are manipulated in specific types of respiratory epithelial cells will be needed to definitively prove a cause-and-effect relationship, these results provide, at the very least, a suggestive link between respiratory epithelial cell proteinopathy, autophagy, and the fibrotic response in the lung.

There are at least two other reasons that a model with spontaneous fibrosis characterized by easily measurable outcomes represents an important advance for the field. First, the model can presumably be used to advance understanding of the mechanism by which epithelial cytotoxicity leads to lung fibrosis. This study does not address potential mechanisms, but several clues are suggested by previous results from accumulation of misfolded ATZ in the liver, including TGFβ and its downstream target connective tissue growth factor (13, 14). These pathways have been previously implicated in lung fibrosis due to epithelial proteotoxicity (23, 54, 55) and in the mechanism of fibrosis in numerous other tissues (56).

Second, the model provides a powerful tool for testing potential therapeutic strategies for pulmonary fibrosis. In this report, for example, we investigated the possibility that therapeutic strategies that enhance autophagy could reverse pulmonary fibrosis. Analyses of lung collagen deposition, leukocyte infiltration, and pulmonary function were used to test two strategies. Systemic administration of drugs that enhance autophagy, CBZ and Flu, decreased lung collagen deposition, leukocyte infiltration, and pulmonary function. Activation of autophagy by lung-directed expression of transcription factor TFEB using helper-dependent adenoviral gene delivery also had a remarkable effect, reversing all of the markers of pulmonary fibrosis. These results are important because they indicate that autophagy in the lungs themselves counteracts the fibrotic process. The salutary effects of CBZ and Flu are particularly important because these drugs are Food and Drug Administration-

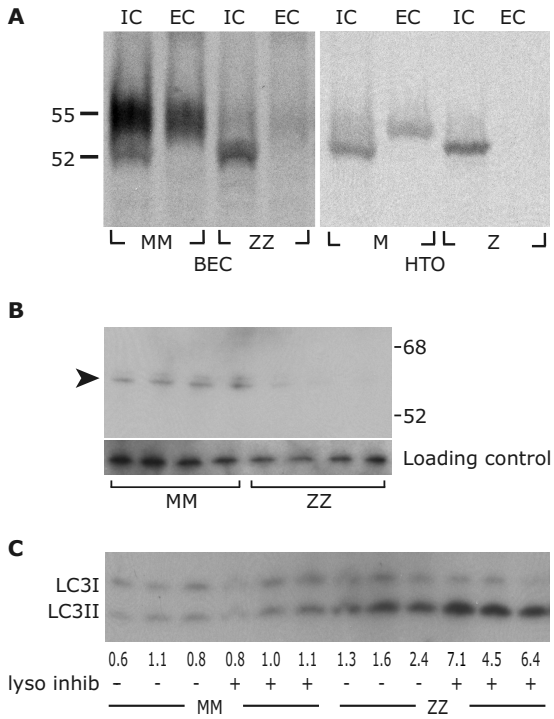

FIGURE 8. **Expression of ATZ and activation of autophagy in BECs from human with ATD.** *A*, BECs from lung of ATD patient (*ZZ*) and control (*MM*) were subjected to pulse-radiolabeling for 2 h and a chase period of 2 h. Samples from HTO/Z (*Z*) and HTO/M (*M*) cell lines were used as controls for intracellular lysates (*IC*) and extracellular fluid respectively (*HTO*). The 52- and 55-kDa forms of AT are indicated by the *tick marks* at the *left*. *EC*, extracellular fluid. *B*, BECs from the ATD patient (*ZZ*) and control (*MM*) were harvested for assay of p62 levels and loading control (*β*-actin) by immunoblot analysis. *C*, BECS from the ATD patient (*ZZ*) and control (*MM*) were incubated in the absence or presence of lysosomal enzyme inhibitors for 4 h and then harvested for LC3 immunoblot analysis. The LC3-II:LC3-I ratio was as follows in the 4 groups: 1.02 in MM, 1.14 in MM with lysosomal inhibitors (*lyso inhib*), 1.85 in ZZ, 4.06 in ZZ with lysosomal inhibitors. Loading control is not necessary because the lanes are being compared for ratio of two bands.

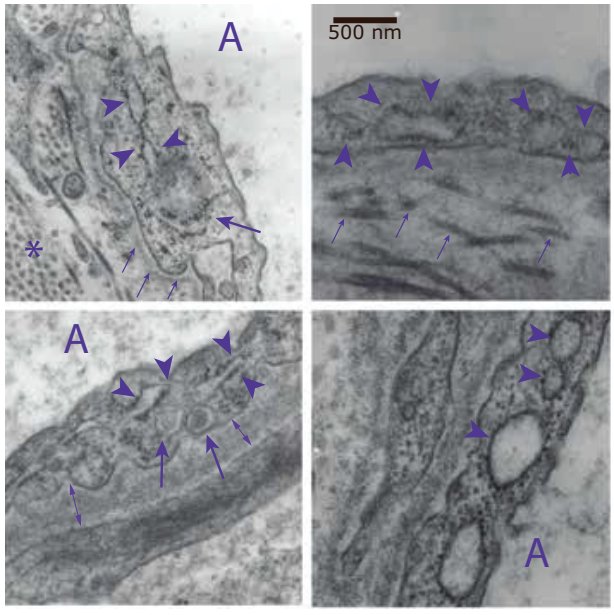

FIGURE 9. **TEM imaging of lung epithelial cells in ATD patients.** *Large arrowheads* point to dilated endoplasmic reticulum, and *arrows* point to autophagosomes. *Small arrows* point to collagen fibers in basement membrane. *Double arrows* point to increased thickness of basement membrane. The *asterisk* points to collagen deposition. *A* orients to air surface.

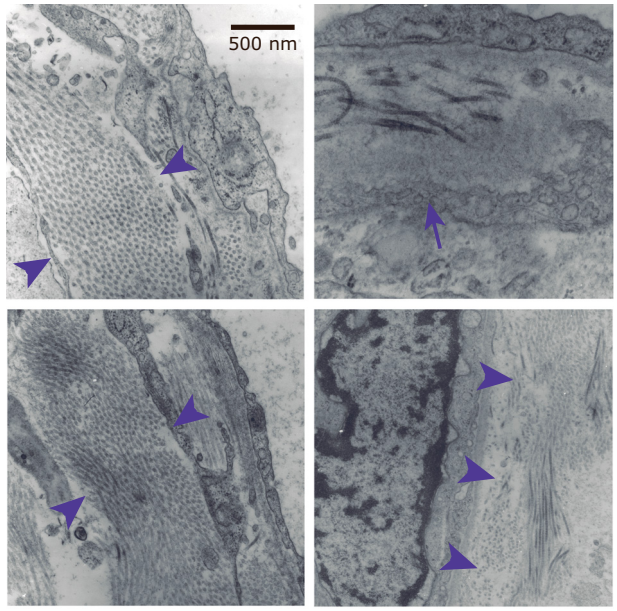

FIGURE 10. **TEM imaging of lung interstitium in ATD patients.** *Arrowheads* point to bundles of collagen, and *arrow* points to collagen fibers within the basement membrane.

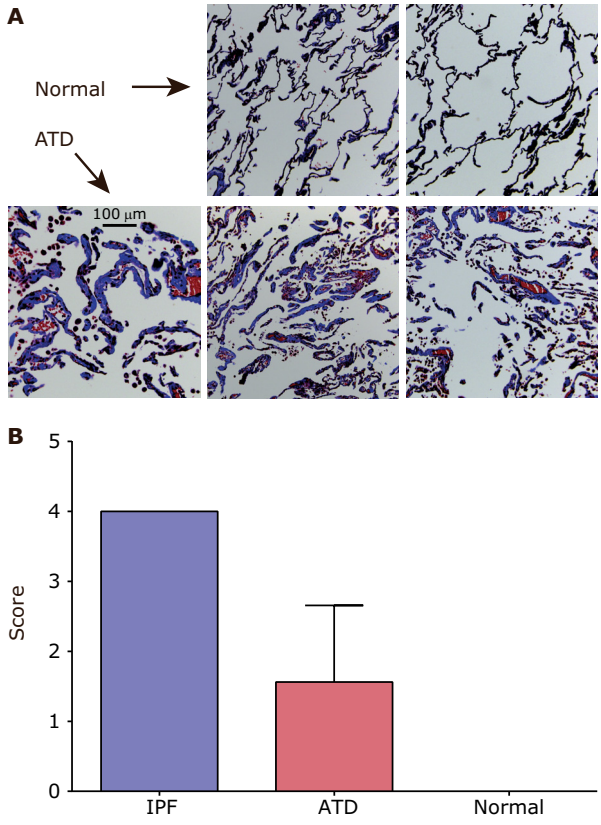

FIGURE 11. **Trichrome staining (*blue*) of human lung specimens.** *A*, sections from the lungs of two normal controls are shown in the *upper panels* and from three ATD patients are shown in the *lower panels*. *B*, scoring from blinded pathological ranking of the degree of trichrome staining for lung tissue specimens from idiopathic pulmonary fibrosis ($n = 3$), ATD ($n = 16$), and normal ($n = 9$). Scores for ATD were significantly greater than normal, $p = 0.0118$.

approved for other clinical purposes, and so the results in the PiZ mouse provide preclinical validation sufficient to move immediately into phase II/III clinical trials for some devastating diseases.

The results also provide further evidence for considering autophagy enhancer therapy for other proteinopathies, especially as autophagy appears to counteract fibrosis from another hepatic proteinopathy and fibrinogen storage disease (57) as well as cardiac and skeletal muscle proteinopathies (3, 10).

We also used human lung cells and tissue specimens to determine whether the PiZ mouse models, something that occurs in the human disease ATD. Significant expression of AT is apparent in human respiratory epithelial cells (Fig. 7), and misfolded ATZ accumulates within respiratory epithelium from patients with ATD (Fig. 8). Although expression of AT and misfolded ATZ in respiratory epithelial cells may be less than in liver cells, the accumulation of ATZ in bronchial epithelial cells, as the only accessible model of human respiratory epithelial cells from ATD patients, was sufficient to activate a marked autophagic response (Fig. 8). The results also show significant collagen deposition in the lungs of patients with ATD (Figs. 9 and 10). Fibrosis has rarely been mentioned in the pathological studies of the lung in ATD (47), but trichrome staining has not been done in lung specimens from this population.[3] Using trichrome staining and blinded pathological analysis, excess collagen deposition was found in 13 of 16 ATD lung specimens (Fig. 11), and marked deposition of collagen was detected by TEM in the lungs of 6 patients with severe ATD lung disease (Fig. 10). Furthermore, careful and sophisticated techniques have been needed to discover that some patients with common forms of COPD have co-existing fibrotic pathology (48–50). However, our study has a relatively small sample size, and the fibrosis we detected in human ATD lung specimens could be due to other causes including cigarette smoking and bronchiectasis, both of which are known to be issues in patients with ATD for whom lung tissue is available. Thus, the results of this study do not meet the criteria of establishing a link between respiratory proteinopathy and lung fibrotic disease in ATD.

It is also important to point out what the PiZ mouse does not represent as a model system. We know that the major pathological and physiological characteristics of the lung in ATD are obstructive in nature, and there is abundant evidence that this is related to loss-of-antiprotease function. Because the PiZ mice have endogenous anti-elastases, they cannot, by definition, manifest loss-of-function for AT. Furthermore, we did not detect any emphysematous changes in the lungs of the PiZ mouse and neither elastase nor cigarette smoking challenge could elicit emphysema-like pathology in this mouse. Rather, the data reported here indicate that PiZ mice model only gain-of-function effects that evolve from respiratory epithelial cell proteinopathy and merely suggest the possibility that these gain-of-function effects are contributing factors to lung disease in humans with ATD that is predominated by emphysema pathology from the loss-of-antiprotease function mechanism. Proteinopathy could theoretically constitute one of the factors that has prevented AT replacement therapy from completely arresting the progression of ATD lung disease even though it corrects the loss-of-antiprotease function (58–65). If gain-of-function proteotoxic mechanism is eventually shown to contribute to lung disease in ATD, we suspect it would only affect a subgroup. We know that only a subgroup of ATD patients get liver disease, which is purely caused by the gain-of-function proteotoxic mechanism (1, 66). In this study we found particularly significant collagen deposition in 4 of 16 ATD lung specimens. Presumably this subgroup is characterized by genetic and/or environmental modifiers that lead to an exaggerated fibrotic response or impair the function of pathways responsible for intracellular disposal of misfolded proteins (53, 67).

Previous studies have introduced the notion that gain-of-function mechanisms may be responsible for some of the lung pathology in ATD, specifically leukocyte infiltration (68, 69). Several groups have theorized that neutrophils are attracted into the lung by polymerized ATZ deposited in the lung interstitium and that the neutrophilic inflammatory effects increase the severity of lung disease. In support of this theory, ATZ polymers, which are known to be chemotactic for neutrophils, have been found in ATD lung and furthermore that the ATZ polymers co-localize with neutrophils in the alveoli of ATD specimens (70). This theory is entirely consistent with the well known abundance of neutrophils and neutrophil effectors such as leukotriene B4 and IL-8 in bronchoalveolar lavage fluid in ATD (71, 72). The ATZ polymers could diffuse from either the blood or body fluids, but local production has been implicated by the finding of ATZ polymers in the bronchoalveolar lavage fluid of a patient with ATD after liver transplantation (73). Because normal AT was present in the blood of this patient, the mutant ATZ in the lung fluid would likely have been produced locally. The results of our study, using a model system that is purely affected by gain-of-function, suggest that leukocyte infiltration of the lungs is due to epithelial cell proteotoxicity because it is reversed when the epithelial load of misfolded ATZ is reduced by pharmacological or genetic manipulation that enhances autophagy. However, further studies are necessary to address this distinction, and it is entirely possible that both mechanisms, leukocyte chemotaxis-mediated by ATZ deposition or by the effects of respiratory epithelial cell proteotoxicity, play roles as additional factors in the lung pathology of ATD.

In summary, the studies reported here demonstrate that the PiZ mouse is a robust model of spontaneous pulmonary fibrosis due to proteinopathy in respiratory epithelial cells. Drug- and gene-based strategies that enhance autophagy reverse this phenotype and should now be considered for testing in human respiratory proteinopathies and perhaps together with replacement therapy for some patients with lung disease due to ATD.

Author Contributions—T. H. and D. H. P. conceived and coordinated the study and wrote the paper. S. C. P. and G. A. S. designed and analyzed the experiments in Fig. 6. D. B. S. and S. A. Y. designed, performed, and analyzed histological specimens. J. F. A. designed, performed, and analyzed the pulmonary function tests. J. W. designed, performed, and analyzed the studies in Figs. 1 and 7. A. S. L. and S. D. S. designed, performed, and analyzed the studies in Fig. 4. P. H., M. E., E. A. G., and H. C. provided technical assistance and contributed to the preparation of the figures. N. P., P. A., and N. B.-P. designed and analyzed the studies in Fig. 5. A. M. H., N. K., and J. P. designed and analyzed the studies in Figs. 9–11. All authors reviewed the results and approved the final version of the manuscript.

[3] J. Tomashefski, personal communication.

Acknowledgments—We are grateful to Drs Geoff Kurland and Daniel Weiner for advice on interpretation of pulmonary function studies.

References

1. Perlmutter, D. H. (2011) α-1-Antitrypsin deficiency: importance of proteasomal and autophagic degradative pathways in disposal of liver disease-associated protein aggregates. *Annu. Rev. Med.* **62,** 333–345
2. Doppler, K., Mittelbronn, M., Lindner, A., and Bornemann, A. (2009) Basement membrane remodeling and segmental fibrosis in sporadic inclusion body myositis. *Neuromuscul. Disord.* **19,** 406–411
3. Bhuiyan, M. S., Pattison, J. S., Osinska, H., James, J., Gulick, J., McLendon, P. M., Hill, J. A., Sadoshima J., and Robbins J. (2013) Enhanced autophagy ameliorates cardiac proteinopathy. *J. Clin. Invest.* **123,** 5284–5297
4. Zhong, Q., Zhou, B., Ann, D. K., Minoo, P., Liu, Y., Banfalvi, A., Krishnaveni, M. S., Dubourd, M., Demaio, L., Willis, B. C., Kim, K. J., duBois, R. M., Crandall, E. D., Beers, M. F., and Borok, Z. (2011) Role of endoplasmic reticulum stress in epithelial-mesenchymal transition of alveolar epithelial cells: effects of misfolded surfactant protein. *Am. J. Respir. Cell Mol. Biol.* **45,** 498–509
5. Lawson, W. E., Cheng, D. S., Degryse, A. L., Tanjore, H., Polosukhin, V. V., Xu, X. C., Newcomb, D. C., Jones, B. R., Roldan, J., Lane, K. B., Morrisey, E. E., Beers, M. F., Yull, F. E., and Blackwell, T. S. (2011) Endoplasmic reticulum stress enhances fibrotic remodeling in the lungs. *Proc. Natl. Acad. Sci. U.S.A.* **108,** 10562–10567
6. Bridges, J. P., Wert, S. E., Nogee, L. M., and Weaver, T. E. (2003) Expression of a human surfactant protein C mutation associated with interstitial lung disease disrupts lung development in transgenic mice. *J. Biol. Chem.* **278,** 52739–52746
7. Guttentag, S. H., Akhtar, A., Tao, J. Q., Atochina, E., Rusiniak, M. E., Swank, R. T., *and* Bates, S. R. (2005) Defective surfactant secretion in a mouse model of Hermansky-Pudlak syndrome. *Am. J. Respir. Cell Mol. Biol.* **33,** 14–21
8. Young, L. R., Gulleman, P. M., Bridges, J. P., Weaver, T. E., Deutsch, G. H., Blackwell, T. S., and McCormack, F. X. (2012) The alveolar epithelium determines susceptibility to lung fibrosis in Hermansky-Pudlak syndrome. *Am. J. Respir. Crit. Care Med.* **186,** 1014–1024
9. Hidvegi, T., Ewing, M., Hale, P., Dippold, C., Beckett, C., Kemp, C., Maurice, N., Mukherjee, A., Goldbach, C., Watkins, S., Michalopoulos, G., and Perlmutter, D. H. (2010) An autophagy-enhancing drug promotes degradation of mutant α1-antitrypsin Z and reduces hepatic fibrosis. *Science* **329,** 229–232
10. Nogalska, A., D'Agostino, C., Terracciano, C., Engel, W. K., and Askanas, V. (2010) Impaired autophagy in sporadic inclusion-body myositis and in endoplasmic reticulum stress-provoked cultured human muscle fibers. *Am. J. Pathol.* **177,** 1377–1387
11. Silverman, E. K., and Sandhaus, R. A. (2009) Clinical practice: α-1-antitrypsin deficiency. *N. Engl. J. Med.* **360,** 2749–2757
12. Kamimoto, T., Shoji, S., Hidvegi, T., Mizushima, N., Umebayashi, K., Perlmutter, D. H., and Yoshimori, T. (2006) Intracellular inclusions containing mutant α1-antitrypsin Z are propagated in the absence of autophagic activity. *J. Biol. Chem.* **281,** 4467–4476
13. Hidvegi, T., Schmidt, B. Z., Hale, P., and Perlmutter, D. H. (2005) Accumulation of mutant α1-antitrypsin Z in the endoplasmic reticulum activates caspases-4 and -12, NFκB and BAP31 but not the unfolded protein response. *J. Biol. Chem.* **280,** 39002–33915
14. Hidvegi, T., Mirnics, K., Hale, P., Ewing, M., Beckett, C., and Perlmutter, D. H. (2007) Regulator of G signaling 16 is a marker for the distinct endoplasmic reticulum stress state associated with aggregated mutant α1-antitrypsin Z in the classical form of α1-antitrypsin deficiency. *J. Biol. Chem.* **282,** 27769–27780
15. Li, J., Pak, S. C., O'Reilly, L. P., Benson, J. A., Wang, Y., Hidvegi, T., Hale, P., Dippold, C., Ewing, M., Silverman, G. A., and Perlmutter, D. H. (2014) Fluphenazine reduces proteotoxicity in *C. elegans* and mammalian models of α-1-antitrypsin deficiency. *PLoS ONE* **9,** e87260
16. Pastore, N., Blomenkamp, K., Annunziata, F., Piccolo, P., Mithbaokar, P., Maria Sepe, R., Vetrini, F., Palmer, D., Ng, P., Polishchuk, E., Iacobacci, S., Polishchuk, R., Teckman, J., Ballabio, A., and Brunetti-Pierri, N. (2013) Gene transfer of master autophagy regulator TFEB results in clearance of toxic protein and corrects hepatic disease in α-1-antitrypsin deficiency. *EMBO Mol. Med.* **5,** 397–412
17. Carlson, J. A., Rogers, B. B., Sifers, R. N., Hawkins, H. K., Finegold, M. J., and Woo, S. L. (1988) Multiple tissues express α 1-antitrypsin in transgenic mice and man. *J. Clin. Invest.* **82,** 26–36
18. Koopman, P., Povey S., and Lovell-Badge, R. H. (1989) Widespread expression of human α1-antitrypsin in transgenic mice revealed by in situ hybridization. *Genes Devel.* **3,** 16–25
19. Wang, D., Haviland, D. L., Burns, A. R., Zsigmond, E., and Wetsel, R. A. (2007) A pure population of lung alveolar epithelial type II cells derived from human embryonic stem cells. *Proc. Natl. Acad. Sci. U.S.A.* **104,** 4449–4454
20. Cichy, J., Potempa, J., and Travis, J. (1997) Biosynthesis of α1-proteinase inhibitor by human lung derived epithelial cells. *J. Biol. Chem.* **272,** 8250–8255
21. Hu, C., and Perlmutter, D. H. (2002) Cell-specific involvement of HNF-1β in α1-antitrypsin gene expression in human respiratory epithelial cells. *Am. J. Physiol. Lung Cell. Mol. Physiol.* **282,** L757–L765
22. Perlmutter, D. H., Cole, F. S., Kilbridge, P., Rossing, T. H., and Colten, H. R. (1985) Expression of the α1-proteinase inhibitor gene in human monocytes and macrophages. *Proc. Natl. Acad. Sci. U.S.A.* **82,** 795–799
23. Blackwell, T. S., Tager, A. M., Borok, Z., Moore, B. B., Schwartz, D. A., Anstrom, K. J., Bar-Joseph, Z., Bitterman, P., Blackburn, M. R., Bradford, W., Brown, K. K., Chapman, H. A., Collard, H. R., Cosgrove, G. P., Deterding, R., Doyle, R., Flaherty, K. R., Garcia, C. K., Hagood, J. S., Henke, C. A., Herzog, E., Hogaboam, C. M., Horowitz, J. C., King, T. E., Jr., Loyd, J. E., Lawson, W. E., Marsh, C. B., Noble, P. W., Noth, I., Sheppard, D., Olsson, J., Ortiz, L. A., O'Riordan, T. G., Oury, T. D., Raghu, G., Roman, J., Sime, P. J., Sisson, T. H., Tschumperlin, D., Violette, S. M., Weaver, T. E., Wells, R. G., White, E. S., Kaminski, N., Martinez, F. J., Wynn, T. A., and Thannickal, V. J., and Eu, J. P. (2014) Future directions in idiopathic pulmonary fibrosis research: an NHLBI workshop report. *Am. J. Respir Crit. Care Med.* **189,** 214–222
24. Komatsu, M., Waguri, S., Ueno, T., Iwata, J., Murata, S., Tanida, I., Ezaki, J., Mizushima, N., Ohsumi, Y., Uchiyama, Y., Kominami, E., Tanaka, K., and Chiba, T. (2005) Impairment of starvation-induced and constitutive autophagy in Atg7-deficient mice. *J. Cell Biol.* **169,** 425–434
25. Maeda, S., Chang, L., Li, Z. W., Luo, J. L., Leffert, H., and Karin, M. (2003) IKKβ is required for prevention of apoptosis mediated by cell-bound but not by circulating TNFα. *Immunity* **19,** 725–737
26. Nakagawa, T., Zhu, H., Morishima, N., Li, E., Xu, J., Yankner, B. A., and Yuan, J. (2000) Caspase-12 mediates endoplasmic reticulum-specific apoptosis and cytotoxicity by amyloid-β. *Nature* **403,** 98–103
27. Yue, Z., Jin, S., Yang, C., Levine, A. J., and Heintz, N. (2003) Beclin 1, an autophagy gene essential for early embryonic development, is a haploinsufficient tumor suppressor. *Proc. Natl. Acad. Sci. U.S.A.* **100,** 15077–15082
28. Messier, E. M., Mason, R. J., and Kosmider, B. (2012) Efficient and rapid isolation and purification of mouse alveolar type II epithelial cells. *Exp Lung Res.* **38,** 363–373
29. Mizushima, N., and Yoshimori, T. (2007) How to interpret LC3 immunoblotting. *Autophagy* **3,** 542–545
30. Pociask, D. A., Scheller, E. V., Mandalapu, S., McHugh, K. J., Enelow, R. I., Fattman, C. L., Kolls, J. K., and Alcorn, J. F. (2013) IL-22 is essential for lung epithelial repair following influenza infection. *Am. J. Pathol.* **182,** 1286–1296
31. Brunetti-Pierri, N., Palmer, D. J., Beaudet, A. L., Carey, K. D., Finegold, M., and Ng, P. (2004) Acute toxicity after high-dose systemic injection of helper-dependent adenoviral vectors into nonhuman primates. *Hum. Gene Ther.* **15,** 35–46
32. Palmer, D., and Ng, P. (2003) Improved system for helper-dependent adenoviral vector production. *Mol. Ther.* **8,** 846–852
33. Suzuki, M., Cela, R., Clarke, C., Bertin, T. K., Mouriño, S., and Lee, B. (2010) Large-scale production of high-quality helper-dependent adenoviral vectors using adherent cells in cell factories. *Hum. Gene Ther.* **21,** 120–126

34. Koehler, D. R., Martin, B., Corey, M., Palmer, D., Ng, P., Tanswell, A. K., and Hu, J. (2006) Readministration of helper-dependent adenovirus to mouse lung. *Gene Ther.* **13,** 773–780
35. Shapiro, S. D., Goldstein, N. M., Houghton, A. M., Kobayashi, D. K., Kelley, D., and Belaaouaj, A. (2003) Neutrophil elastase contributes to cigarette smoke-induced emphysema in mice. *Am. J. Pathol.* **163,** 2329–2335
36. Devor, D. C., Bridges, R. J., and Pilewski, J. M. (2000) Pharmacological modulation of ion transport across wild-type and ΔF508 CFTR-expressing human bronchial epithelia. *Am. J. Physiol. Cell Physiol.* **279,** C461–C479
37. Wang, J., Edeen, K., Manzer, R., Chang, Y., Wang, S., Chen, X., Funk, C. J., Cosgrove, G. P., Fang, X., and Mason, R. J. (2007) Differentiated human alveolar epithelial cells and reversibility of their phenotype *in vitro*. *Am. J. Respir. Cell Mol Biol.* **36,** 661–668
38. Mizushima, N., Yamamoto, A., Matsui, M., Yoshimori, T., and Ohsumi, Y. (2004) *In vivo* analysis of autophagy in response to nutrient starvation using transgenic mice expressing a fluorescent autophagosome marker. *Mol. Biol. Cell* **15,** 1101–1111
39. Qu, X., Yu, J., Bhagat, G., Furuya, N., Hibshoosh, H., Troxel, A., Rosen, J., Eskelinen, E. L., Mizushima, N., Ohsumi, Y., Cattoretti, G., and Levine, B. (2003) Promotion of tumorigenesis by heterozygous disruption of the beclin 1 autophagy gene. *J. Clin. Invest.* **112,** 1809–1820
40. Zhou, Z., Song, R., Fattman, C. L., Greenhill, S., Alber, S., Oury, T. D., Choi, A. M., and Morse, D. (2005) Carbon monoxide suppresses bleomycin-induced lung fibrosis. *Am. J. Pathol.* **166,** 27–37
41. O'Donnell, D. E., and Fitzpatrick, M. F. (2003) Physiology of interstitial lung disease. In *Interstitial Lung Disease* (Schwarz, M. I., and King, T. E., eds) 4th Ed., pp. 54–74, BC Decker, Hamilton, Ontario, Canada
42. Fulmer, J. D., Roberts, W. C., von Gal, E. R., and Grystal, R. G. (1977) Small airways in idiopathic pulmonary fibrosis: comparison of morphologic and physiologic observations. *J. Clin. Invest.* **60,** 595–610
43. Lovgren, A. K., Jania, L. A., Hartney, J. M., Parsons, K. K., Audoly, L. P., Fitzgerald, G. A., Tilley, S. L., and Koller, B. H. (2006) COX-2-derived prostacyclin protects against bleomycin-induced pulmonary fibrosis. *Am. J. Physiol. Lung Cell. Mol. Physiol.* **291,** L144–LL156
44. Dackor, R. T., Cheng, J., Voltz, J. W., Card, J. W., Ferguson, C. D., Garrett, R. C., Bradbury, J. A., DeGraff, L. M., Lih, F. B., Tomer, K. B., Flake, G. P., Travlos, G. S., Ramsey, R. W., Jr., Edin, M. L., Morgan, D. L., and Zeldin, D. C. (2011) Prostaglandin E2 protects murine lungs from bleomycin-induced pulmonary fibrosis and lung dysfunction. *Am. J. Physiol. Lung Cell. Mol. Physiol.* **301,** L645–L655
45. Ding, Q., Cai, G. Q., Hu, M., Yang, Y., Zheng, A., Tang, Q., Gladson, C. L., Hayasaka, H., Wu, H., You, Z., Southern, B. D., Grove, L. M., Rahaman, S. O., Fang, H., and Olman, M. A. (2013) FAK-related non-kinase is a multifunctional negative regulator of pulmonary fibrosis. *Am. J. Pathol.* **182,** 1572–1584
46. Settembre, C., Di Malta, C., Polito, V. A., Garcia Arencibia, M., Vetrini, F., Erdin, S., Erdin, S. U., Huynh, T., Medina, D., Colella, P., Sardiello, M., Rubinsztein, D. C., and Ballabio, A. (2011) TFEB links autophagy to lysosomal biogenesis. *Science* **332,** 1429–1433
47. Tomashefski, J. F., Jr., Crystal, R. G., Wiedemann, H. P., Mascha, E., Stoller, J. K., Alpha 1-Antitrypsin Deficiency Registry Study Group (2004) The bronchopulmonary pathology of anti-1-antitrypsin (AAT) deficiency: findings of the death review committee of the national registry for individuals with severe deficiency of α-1-antitrypsin. *Hum. Pathol.* **35,** 1452–1461
48. King, T. E. (2011) Smoking and subclinical interstitial lung disease. *N. Engl. J. Med.* **364,** 968–970
49. Vlahovic, G., Russell, M. L., Mercer, R. R., and Crapo, J. D. (1999) Cellular and connective tissue changes in alveolar septal walls in emphysema. *Am. J. Resp Crit. Care Med.* **160,** 2086–2092
50. Washko, G. R., Hunninghake, G. M., Fernandez, I. E., Nishino, M., Okajima, Y., Yamashiro, T., Ross, J. C., Estépar, R. S., Lynch, D. A., Brehm, J. M., Andriole, K. P., Diaz, A. A., Khorasani, R., D'Aco, K., Sciurba, F. C., Silverman, E. K., Hatabu, H., and Rosas, I. O., COPDGene Investigators (2011) Lung volumes and emphysema in smokers with interstitial lung abnormalities. *N. Engl. J. Med.* **364,** 897–906
51. Wang, Y., Kuan, P. J., Xing, C., Cronkhite, J. T., Torres, F., Rosenblatt, R. L., DiMaio, J. M., Kinch, L. N., Grishin, N. V., and Garcia, C. K. (2009) Genetic defects in surfactant protein A2 are associated with pulmonary fibrosis and lung cancer. *Am. J. Hum. Genet.* **84,** 52–59
52. Lawson, W. E., Polosukhin, V. V., Stathopoulos, G. T., Zoia, O., Han, W., Lane, K. B., Li, B., Donnelly, E. F., Holburn, G. E., Lewis, K. G., Collins, R. D., Hull, W. M., Glasser, S. W., Whitsett, J. A., and Blackwell, T. S. (2005) Increased and prolonged pulmonary fibrosis in surfactant protein C-deficient mice following intratracheal bleomycin. *Am. J. Pathol.* **167,** 1267–1277
53. Long, O. S., Benson, J. A., Kwak, J. H., Luke, C. J., Gosai, S. J., O'Reilly, L. P., Wang, Y., Li, J., Vetica, A. C., Miedel, M. T., Stolz D. B., Watkins, S. C., Züchner, S., Perlmutter, D. H., Silverman, G. A., and Pak, S. C. (2014) A *C. elegans* model of human α1-antitrypsin deficiency links components of the RNAi pathway to misfolded protein turnover. *Hum. Mol. Genet.* **23,** 5109–5122
54. DeMaio, L., Buckley, S. T., Krishnaveni, M. S., Flodby, P., Dubourd, M., Banfalvi, A., Xing, Y., Ehrhardt, C., Minoo, P., Zhou, B., Crandall, E. D., and Borok, Z. (2012) Ligand-independent transforming growth factor-β type I receptor signaling mediates type I collagen-induced epithelial mesenchymal transition. *J. Pathol.* **226,** 633–644
55. Tanjore, H., Cheng, D.-S., Degryse, A. L., Zoz, D. F., Abdolrasulnia, R., Lawson, W. E., Blackwell, T. S. (2011) Alveolar epithelial cells undergo epithelial-to-mesenchymal transition in response to endoplasmic reticulum stress. *J. Biol. Chem.* **286,** 30972–30980
56. Rockey, D. C., Bell, P. D., and Hill, J. A. (2015) Fibrosis: a common pathway to organ injury and failure. *N. Engl. J. Med.* **372,** 1138–1149
57. Puls, F., Goldschmidt, I., Bantel, H., Agne, C., Bröcker, V., Dämmrich, M., Lehmann, U., Berrang, J., Pfister, E. D., Kreipe, H. H., and Baumann, U. (2013) Autophagy-enhancing drug carbamazepine diminishes hepatocellular death in fibrinogen storage disease. *J Hepatol.* **59,** 626–630
58. Demeo, D. L., Sandhaus, R. A., Barker, A. F., Brantly, M. L., Eden, E., McElvaney, N. G., Rennard, S., Burchard, E., Stocks, J. M., Stoller, J. K., Strange, C., Turino, G. M., Campbell, E. J., and Silverman, E. K. (2007) Determinants of airflow obstruction in severe α-1-antitrypsin deficiency. *Thorax* **62,** 806–813
59. Wencker, M., Fuhrmann, B., Banik, N., and Konietzko, N., Wissenschaftliche Arbeitsgemeinschaft zur Therapie von Lungenerkrankungen (2001) Longitudinal follow-up of patients with α1-protease inhibitor deficiency before or during therapy with IV α1-protease inhibitor. *Chest* **119,** 737–744
60. Dirksen, A., Piitulainen, E., Parr, D. G., Deng, C., Wencker, M., Shaker, S. B., and Stockley, R. A. (2009) Exploring the role of CT densitometry: a randomized study of augmentation therapy in α1-antitrypsin deficiency. *Eur. Respir J.* **33,** 1345–1353
61. Gotzsche, P. C., and Johansen, H. K. (2010) Intravenous α-1-antitrypsin augmentation therapy for treating patients with α-1-antitrypsin deficiency and lung disease. *Cochrane Database Syst. Rev.* 10.1002/14651858.CDOO7851.pub2
62. Tanash, H. A., Riise, G. C., Hansson, L., Nilsson, P. M., and Piitulainen, E.(2011) Survival benefit of lung transplantation in individuals with severe α1-antitrypsin deficiency (PiZZ) and emphysema. *J. Heart Lung Transplant* **30,** 1342–1347
63. Strange, C., Stoller, J. K., Sandhaus, R. A., Dickson, R., and Turino, G. (2006) Results of a survey of patients with α-1-antitrypsin deficiency. *Respiration* **73,** 185–190
64. Christie, J. D., Edwards, L. B., Kucheryavaya, A. Y., Benden, C., Dipchand, A. I., Dobbels, F., Kirk, R., Rahmel, A. O., Stehlik, J., and Hertz, M. I., International Society of Heart and Lung Transplantation (2012) The registry of the international society for heart and lung transplantation: 29th adult lung and heart-lung transplant report-2012. *J. Heart Lung Transplant* **31,** 1073–1086
65. Carey, E. J., Iyer, V. N., Nelson, D. R., Nguyen, J. H., and Krowka, M. J. (2013) Outcomes for recipients of liver transplantation for α-1-antitrypsin deficiency-related cirrhosis. *Liver Transpl.* **19,** 1370–1376
66. Piitulainen, E., Carlson, J., Ohlsson, K., and Sveger, T. (2005) α-1-Antitrypsin deficiency in 26-year-old subjects: lung, liver and protease-protease inhibitor studies. *Chest* **128,** 2076–2081
67. Tafaleng, E. N., Chakraborty, S., Han, B., Hale, P., Wu, W., Soto-Gutierrez,

A., Feghali-Bostwick, C. A., Wilson, A. A., Kotton, D. N., Nagaya, M., Strom, S. C., Roy-Chowdhury J., Stolz, D. B., Perlmutter, D. H., and Fox, I. J. (2015) Induced pluripotent stem cells model personalized variations in liver disease due to α1-antitrypsin deficiency. *Hepatology* **62,** 147–157

68. Dickens, J. A., and Lomas, D. A. (2011) Why has it been so difficult to prove the efficacy of α-1-antitrypsin replacement therapy? Insights from the study of disease pathogenesis. *Drug Des. Devel. Ther.* **5,** 391–405
69. Elliott, P. R., Bilton, D., and Lomas, D. A. (1998) Lung polymers in Z α1-antitrypsin deficiency-related emphysema. *Am. J. Respir. Cell Mol. Biol.* **18,** 670–674
70. Mahadeva, R., Atkinson, C., Li, Z., Stewart, S., Janciauskiene, S., Kelley, D. G., Parmar, J., Pitman, R., Shapiro, S. D., and Lomas, D. A. (2005) Polymers of Z α1-antitrypsin co-localize with neutrophils in emphysematous alveoli and are chemotactic *in vivo*. *Am. J. Pathol.* **166,** 377–386
71. Hubbard, R. C., Fells, G., Gadek, J., Pacholok, S., Humes, J., and Crystal, R. G.(1991) Neutrophil accumulation in the lung in α1-antitrypsin deficiency: spontaneous release of leukotriene B4 by alveolar macrophages. *J. Clin. Invest.* **88,** 891–897
72. Woolhouse, I. S., Bayley, D. L., and Stockley, R. A. (2002) Sputum chemotactic activity in chronic obstructive pulmonary disease: effect of α(1)-antitrypsin deficiency and role of leukotriene B(4) and interleukin 8. *Thorax* **57,** 709–714
73. Mulgrew, A. T., Taggart, C. C., Lawless, M. W., Greene, C. M., Brantly, M. L., O'Neill, S. J., and McElvaney, N. G. (2004) Z α1-antitrypsin polymerizes in the lung and acts as a neutrophil chemoattractant. *Chest* **125,** 1952–1957